

Cisplatin

Crystal Structure of a Cisplatin–(1,3-GTG) Cross-Link within DNA Polymerase η^{**}

Thomas Reißner, Sabine Schneider, Stephanie Schorr, and Thomas Carell*

Dedicated to Dr. Klaus Römer on the occasion of his 70th birthday

Cisplatin (*cis*-diamminedichloroplatinum(II)) is one of the most widely used anticancer agents against ovarian, cervical, head and neck, and non-small-cell lung cancer.^[1] It is one of the few therapeutics able to cure cancer. However, this property is limited to testicular cancer, where overall cure rates of 90 % are reached.^[2,3] Cisplatin exerts its anticancer function by forming stable DNA adducts (Figure 1).^[1,4–6] The major adducts are 1,2-intrastrand cross-links (Pt–GG (**1**), 47–50 %; Pt–AG, 23–28 %) and 1,3-intrastrand cross-links (Pt–GNG, 8–10 %) between two guanines separated by another base.^[6–8] It was recently shown that the 1,2-cross-link **1** is tolerated by cells. Two specialized polymerases (Pol η and Pol ζ) act in concert to enable cells to bypass lesion **1** during replication. The complex process is initiated by Pol η , which inserts a correct dC opposite the lesion. Pol ζ subsequently extends this structure to achieve full bypass. This process

counteracts the therapeutic effect of cisplatin and contributes to tumor resistance.^[9] Currently it is believed that the 1,3-cross-links are stronger replication blocks and hence more cytotoxic.^[10,11]

Here we report that yeast Pol η pairs the Pt–GTG lesion with two nucleobases, thereby enabling partial bypass. We provide crystallographic data on a Pt–GTG lesion (**2**) inside the polymerase, which allows us to explain the mechanism of the partial bypass reaction.^[12–15] For the study we prepared the DNA template strand **3** containing a single site-specific (1,3-GTG)–cisplatin intrastrand cross-link. To this end, a small DNA oligomer with an isolated GTG sequence was treated with activated cisplatin.^[16] The DNA strand containing the Pt–GTG lesion was isolated using anion-exchange HPLC followed by reversed-phase HPLC. The two-step isolation/purification protocol furnished the Pt–GTG-lesion-containing oligonucleotide **3** in purities of above 98 %.^[17] To study lesion bypass by Pol η , primer extension assays were performed (Figure 2).

The Pt–GTG-lesion-containing 18mer DNA strand **3**, and as a control the same strand without the Pt–GTG lesion were annealed to a 5'-fluorescein-labeled DNA primer. The two DNA constructs were incubated with purified Pol η from *Saccharomyces cerevisiae* at concentrations of 1–1000 nM in the presence of initially all four nucleotide triphosphates (Figure 2a), and the reactions were analyzed by gel electrophoresis. Pol η fully extends the lesion-free DNA template (Figure 2a), but full extension of the template containing the Pt–GTG is not possible, in agreement with recent data from human Pol η .^[18] Yeast Pol η incorporates one base efficiently opposite the lesion and a second base under forcing conditions.

We next determined which base Pol η inserts during the partial bypass reaction. To this end, we added the triphosphates individually to the primer extension reaction (Figure 2b,c). The data show that the enzyme correctly inserts a dC base opposite the 3'dG part of the Pt–GTG lesion. The second nucleotidyl transfer is much slower (Figure 2c) but clearly observed at higher enzyme concentrations (350 nM, Figure 2c, right). In this step the enzyme incorporates either dA or dG with a preference for dG. It has been shown previously that the yeast enzyme favors incorporation of dG over dA when reading through an abasic site, because of the better stacking properties of dG.^[19] After this second elongation step, the enzyme is blocked (Figure 2a).

To examine the mechanism that enables Pol η to incorporate two bases opposite a three-nucleobase Pt–GTG lesion, we crystallized Pol η from *S. cerevisiae* together with a

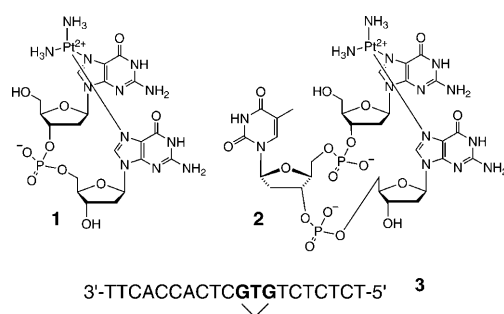


Figure 1. Structure of the cisplatin–(1,2-GG) lesion **1** and of the cisplatin–(1,3-GTG) lesion **2**. Depiction of the DNA sequence **3** containing the lesion **2**.

[*] T. Reißner,^[‡] Dr. S. Schneider,^[‡] S. Schorr, Prof. Dr. T. Carell
Center for Integrated Protein Science (CiPS^M)
Department of Chemistry, Ludwig-Maximilians-University
Butenandtstrasse 5–13, 81377 Munich (Germany)
Fax: (+49) 89-2180-77756
E-mail: thomas.carell@cup.uni-muenchen.de
Homepage: <http://www.carellgroup.de>

[†] These authors contributed equally to this work.

[**] We thank the excellence cluster CiPS^M, SFB 646, and SFB 749 for generous support. T.R. is grateful to the Boehringer Ingelheim Foundation for a predoctoral fellowship. S. Schorr thanks the Verband der chemischen Industrie (VCI) for a Kekulé Fellowship. We also thank the beamline scientists at the ESRF and SLS for their support in setting up the beamlines.

Supporting information for this article is available on the WWW under <http://dx.doi.org/10.1002/anie.201000414>.

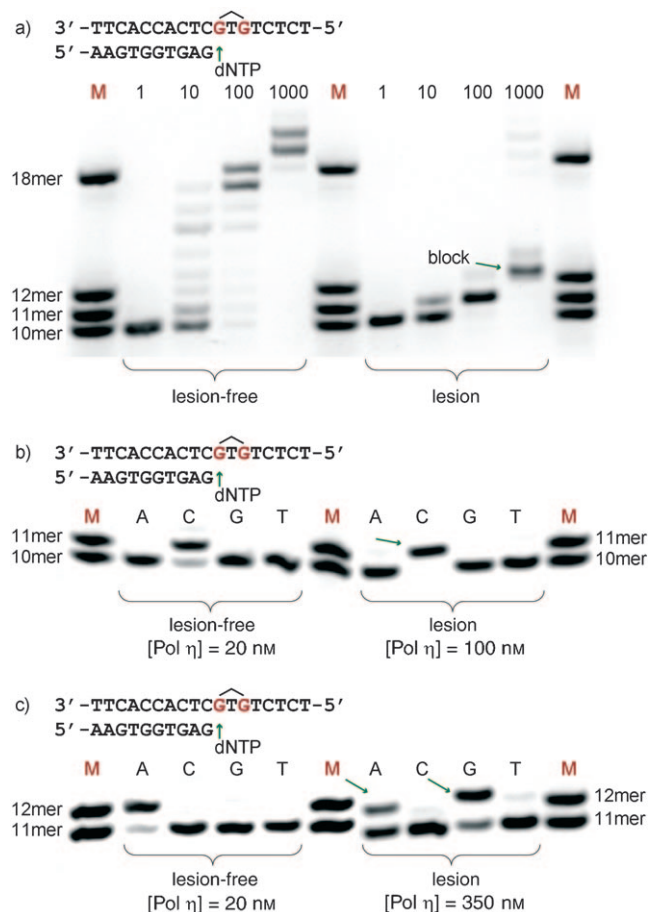


Figure 2. Primer extension reaction with Pol η and fluorescence-labeled primers. a) Primer extension dependent on enzyme concentration; final concentrations of 1–1000 nM Pol η were used with an excess of substrate (10 μ M template DNA and 100 μ M nucleotide triphosphates) in 10 mM Tris-HCl, 50 mM NaCl, 10 mM MgCl₂, 1 mM dithiothreitol (DTT), pH 7.9. b) Correct incorporation of dC opposite the 3'dG of Pt-GTG. c) Selectivity of the nucleotide insertion process opposite the central dT of the lesion (incorporation of either a dA or a dG).

template-primer complex containing a Pt-GTG lesion in the second elongation step. For the experiment the primer was designed to end with a 2',3'-dideoxycytosine directly opposite the 3'dG of the Pt-GTG in order to prevent further elongation by the polymerase. Crystallizations were set up with dATP in the precipitant solution. Crystals of the enzyme in complex with Pt-GTG and dATP in the active site diffracted X-rays to 2.5 Å spacing (for detailed information about data collection and processing, and structure refinement see the Supporting Information and Table S1). The structure was solved by combining the experimental Pt-SAD phases (SAD = single-wavelength anomalous dispersion) with phases obtained through molecular replacement with the apo enzyme.^[20]

Figure 3a depicts a schematic representation of the complex structure, showing the fold of a polydactyl right hand typical for the Y-family polymerases, with the additional polymerase-associated domain (PAD) mimicking a set of extra fingers.^[20] An example of the electron density of the Pt-GTG lesion is shown in Figure 3b. In the asymmetric unit of

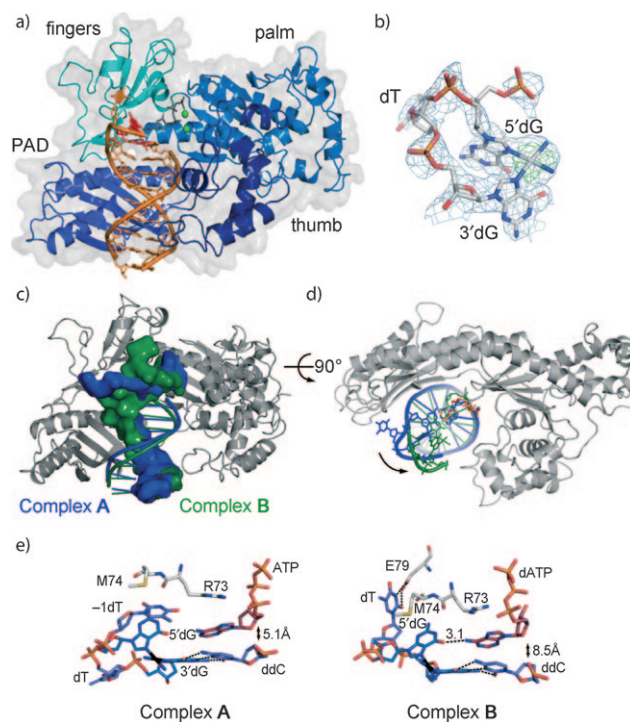


Figure 3. Crystal structure of a (DNA template)-primer duplex containing a cisplatin-(1,3-GTG) lesion in complex with Pol η . a) Schematic representation of the overall structure with the protein depicted as ribbon model. The lesion and dATP are shown as red and gray stick models, respectively. The two Ca²⁺ ions essential for catalysis are represented as green spheres. b) Electron density map ($F_{\text{obs}} - D F_{\text{calc}}$) of the Pt-GTG lesion (complex B) contoured at 2 σ level (blue); the anomalous-difference Fourier electron density map of the platinum atom (3 σ) is overlaid in green; the two guanines of the lesion are fixed with an internal angle of approximately 70°. c) Rotation of the DNA by about one nucleotide into the active site, with complex A in blue, complex B in green. d) View 90° rotated; for clarity the finger domain was removed from the ribbon representation. e) Detailed view of the active sites. The 3'dG of the lesion forms a Watson-Crick base pair with the ddC end of the primer, with R73 stacking on top of the incoming ATP. In complex B the DNA is further rotated into the active site of the enzyme, with Glu79 hydrogen bonding to the central unstacked thymine of the lesion. The 5'dG forms a hydrogen bond with the ATP. This, however, leads to an increase of the distance between a modeled hydroxy group and the nucleotide in the active site from 5.1 Å to 8.1 Å.

the crystal two different complexes, complex A and complex B, were found, in which the DNA-primer complex is in different conformations (Figure 3c,d). Met74 resides between the nucleotides -2 (dC) and -1 (dT) 5' of the Pt-GTG lesion in complex A. In complex B this methionine is positioned between the 5' dG of Pt-GTG lesion and the -1 base (dT) because the DNA is rotated by one nucleotide into the active site (Figure 3e). Such sulfur-arene interactions provide a significant amount of stabilizing dispersion energy.^[21] The conserved amino acid Arg73, which is strictly required for translesion synthesis (TLS) because it stabilizes the triphosphate in the active site,^[12] stacks in the absence of a templating base on top of the incoming dATP, holding it in place for nucleophilic attack by the putative primer OH group (Figure 3e and Figure S1 in the Supporting Information).

In both complexes **A** and **B** almost ideal Watson–Crick base-pairing between the ddC 3' primer end and the 3'dG of the lesion (Pt–GTG) is observed (Figure 3e). This perfect Watson–Crick base-pairing is the reason for efficient and correct incorporation of dCTP opposite the 3'dG part of Pt–GTG during the first bypass step. The Pt–GTG cross-link induces a severe distortion of the DNA because the two guanines of the lesion are fixed with an internal angle of roughly 70° (Figure 3b). The most dramatic element observed in the structure is the central thymine of lesion **2**. It is not located between the guanine moieties, but fully extruded from the duplex and partially flexible^[10] (Figure 3). Thus the central dT is unable to guide the second elongation step, which has to occur opposite 5'dG (Pt–GTG). Indeed, in the crystal structure we observe that the incoming dATP interacts with the 5'dG part of the lesion. In addition, the flipped-out central dT of the Pt–GTG lesion hinders any further movement of the polymerase along the template primer complex, explaining why Pol η stalls after the second elongation step. Figure 4 shows the blockage in detail; the protein surface is shown as a transparent grey surface. The central dT of the Pt–GTG lesion is positioned directly in front of the protein so that any further movement of the polymerase along the DNA strand is blocked.

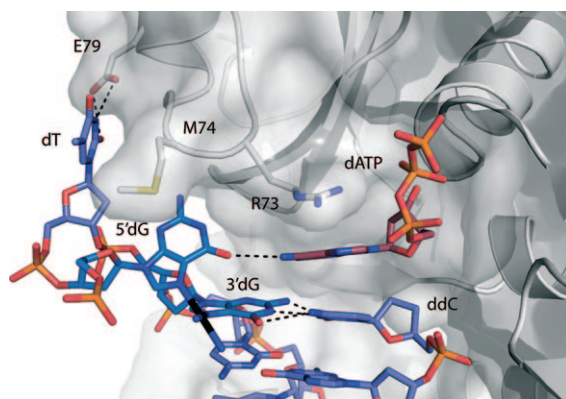


Figure 4. Closeup view of the active site in complex **B**, overlaid with a semitransparent surface representation of the protein. Met74 wedged in between the central dT and 5'dG of the lesion prevents further movement of the polymerase along the DNA template strand.

The structures also explain why the second insertion step is slow. For efficient chemistry, the template–primer complex has to rotate complex **A** to give complex **B** in order to position the primer strand correctly for attack of the triphosphate. This rotation is driven by formation of hydrogen bonds between the incoming triphosphate and the templating base. The rotational movement complex **A**→complex **B** is needed to reduce the distance between the 3'-primer-OH group and the α -phosphate of the dNTP.^[12,22] In complex **B**, we see the template–primer construct in the correct state for nucleotidyl transfer. Indeed a hydrogen bond (3.1 Å) is established between the NH₂(6) of the incoming dATP and O(6) of the 5'dG of the lesion (Figure 3e). Despite this, the distance between the putative primer 3'-OH group and the α -phosphate of the dNTP is not reduced but increased from

5.1 Å (complex **A**) to about 8.5 Å (complex **B**) as a consequence of the strong DNA distortion induced by the cross-link. The second distance is clearly too far for efficient nucleotidyl transfer. For comparison, the distance between the α -phosphate and the modeled 3'OH of the primer is approximately 3.5 Å in the high-fidelity polymerases of the T7 phage^[23] and *Bacillus stearothermophilus*.^[24]

In summary, our data show that the low-fidelity polymerase Pol η is able to place two nucleobases opposite the Pt–GTG lesion and hence enables partial bypass. The crystal structure reveals that the flipped-out central dT of the Pt–GTG cross-link is the critical element that hinders Pol η from performing full bypass. Because of its extruded state, dT cannot be positioned in the active site, thus blocking the movement of the primer–template complex through the polymerase. However, partial-bypassed structures are known substrates for polymerase ζ, and so the partial bypass result reported here suggests that even the strongly helix-disturbing lesions Pt–GNG may be efficiently bypassed in vivo again by the concerted action of Pol η and Pol ζ.

Received: January 23, 2010

Published online: March 23, 2010

Keywords: antitumor agents · cisplatin · DNA damage · polymerases · translesion synthesis

- [1] D. Wang, S. J. Lippard, *Nat. Rev. Drug Discov.* **2005**, *4*, 307–320.
- [2] Y. Jung, S. J. Lippard, *Chem. Rev.* **2007**, *107*, 1387–1407.
- [3] J. Reedijk, *Eur. J. Inorg. Chem.* **2009**, 1303–1312.
- [4] Z. H. Siddik, *Oncogene* **2003**, *22*, 7265–7279.
- [5] H. Zorbas, B. K. Keppler, *ChemBioChem* **2005**, *6*, 1157–1166.
- [6] E. R. Jamieson, S. J. Lippard, *Chem. Rev.* **1999**, *99*, 2467–2498.
- [7] A. E. Egger, C. G. Hartinger, H. B. Hamidane, Y. O. Tsybin, B. K. Keppler, P. J. Dyson, *Inorg. Chem.* **2008**, *47*, 10626–10633.
- [8] A. M. Fichtinger-Schepman, J. L. van der Veer, J. H. den Hartog, P. H. Lohman, J. Reedijk, *Biochemistry* **1985**, *24*, 707–713.
- [9] S. Shachar, O. Ziv, S. Avkin, S. Adar, J. Wittschieben, T. Reissner, S. Chaney, E. C. Friedberg, Z. Wang, T. Carell, N. Geacintov, Z. Livneh, *EMBO J.* **2009**, *28*, 383–394.
- [10] J. M. Teuben, C. Bauer, A. H. Wang, J. Reedijk, *Biochemistry* **1999**, *38*, 12305–12312.
- [11] A. M. Fichtinger-Schepman, H. C. van Dijk-Knijnenburg, S. D. van der Velde-Visser, F. Berends, R. A. Baan, *Carcinogenesis* **1995**, *16*, 2447–2453.
- [12] a) A. Alt, K. Lammens, C. Chiocchini, A. Lammens, J. C. Pieck, D. Kuch, K. P. Hopfner, T. Carell, *Science* **2007**, *318*, 967–970; For the structure of Pt–GG DNA in complex with the yeast RNA Pol II, see: b) G. E. Damsma, A. Alt, F. Brueckner, T. Carell, P. Cramer, *Nat. Struct. Mol. Biol.* **2007**, *14*, 1127–1133.
- [13] E. Bassett, A. Vaisman, J. M. Havener, C. Masutani, F. Hanaoka, S. G. Chaney, *Biochemistry* **2003**, *42*, 14197–14206.
- [14] E. Bassett, A. Vaisman, K. A. Tropea, C. M. McCall, C. Masutani, F. Hanaoka, S. G. Chaney, *DNA Repair* **2002**, *1*, 1003–1016.
- [15] C. Masutani, R. Kusumoto, S. Iwai, F. Hanaoka, *EMBO J.* **2000**, *19*, 3100–3109.
- [16] M. Wei, S. M. Cohen, A. P. Silverman, S. J. Lippard, *J. Biol. Chem.* **2001**, *276*, 38774–38780.
- [17] J. Butenandt, T. Burgdorf, T. Carell, *Synthesis* **1999**, 1085–1105.
- [18] S. Chijiwa, C. Masutani, F. Hanaoka, S. Iwai, I. Kuraoka, *Carcinogenesis* **2010**, *31*, 388–393.

- [19] L. Haracska, M. T. Washington, S. Prakash, L. Prakash, *J. Biol. Chem.* **2001**, 276, 6861–6866.
- [20] J. Trincão, R. E. Johnson, C. R. Escalante, S. Prakash, L. Prakash, A. K. Aggarwal, *Mol. Cell* **2001**, 8, 417–426.
- [21] E. A. Meyer, R. K. Castellano, F. Diederich, *Angew. Chem.* **2003**, 115, 1244–1287; *Angew. Chem. Int. Ed.* **2003**, 42, 1210–1250.
- [22] E. Bassett, N. M. King, M. F. Bryant, S. Hector, L. Pendyala, S. G. Chaney, M. Cordeiro-Stone, *Cancer Res.* **2004**, 64, 6469–6475.
- [23] L. G. Briebe, B. F. Eichman, R. J. Kokoska, S. Doublié, T. A. Kunkel, T. Ellenberger, *EMBO J.* **2004**, 23, 3452–3461.
- [24] G. W. Hsu, J. R. Kiefer, D. Burnouf, O. J. Becherel, R. P. Fuchs, L. S. Beese, *J. Biol. Chem.* **2004**, 279, 50280–50285.
-